

SciEn Conference Series: Engineering Vol. 3, 2025, pp 713-718

https://doi.org/10.38032/scse.2025.3.181

Kinematic Analysis and Comparison of Mechanical Walkers Using Theo Jansen's Mechanism

Kazi S M Jaman Fahim, Asha Rani Shorma, Tauseef Ahmad, Md. Ashraful Islam

Department of Mechanical Engineering, Khulna University of Engineering & Technology, Khulna-9203, Bangladesh

ABSTRACT

A comprehensive kinematic analysis and modeling of four, six, as well as eight-legged mechanical models based on the Theo Jansen mechanism has been conducted in this paper. This locomotion assisted structures are ideal for replacing wheeled robots, which in most cases have a challenge on rough surfaces. Three models were designed and analyzed for motion using Solid Works with specific parameters such as angular velocity and motor torque analyzed. This study shows that walking with an eight-legged configuration is much smoother than that of the four and six-legged configurations. Nonetheless, this benefit is counteracted by the large amounts of materials needed as well as a larger body weight. It provides an effective understanding of the performance of walking, its associated mechanical system, and the material required for the system. The results indicated that more walking legged robots would be more adaptable to the environment and would be a better option than wheeled robots, since the ingenious machines in legs provided more movement in difficult terrain. Such research helps to foster interest in bio-inspired robotics and helps develop better walking mechanisms for non-flat surfaces.

Keywords: Theo Jansen, Kinematics, Bio-inspired, Motion Analysis, Comparison.



Copyright @ All authors

This work is licensed under a Creative Commons Attribution 4.0 International License.

1. Introduction

Theo Jansen's mechanism, an intriguing combination of art and engineering, has been widely recognized for its ability to replicate lifelike walking movements using purely mechanical components. The creations, known as Strandbeest, are inspired by biological locomotion, with a system of interconnected links and joints used to produce smooth and efficient motion. These mechanisms serve as an example of how simple, rigid mechanical systems can be optimized to imitate complex, organic movement without the need for motors or electronics. Applications of the Theo Jansen mechanism include walking robots, art installations, prosthetics, search and rescue, military robotics, educational kits, agriculture, and exploration. Materials such as PVC, aluminum, acrylic, polycarbonate, carbon fiber, and 3D printing materials like PLA or ABS are selected based on weight, strength, and durability when building Theo Jansen robots. Kaval Bhavsar used plastic materials to create an eight-legged robot [2]. Recent works on the Theo Jansen mechanism are related to its kinematic analysis, optimization, and simulation by tools such as Mathematica, MaTX, and Borland's Delphi, but mention that systematic methods must be developed to improve its performance [3]. As a one-degree-of-freedom planar 12-link system, the Jansen mechanism has been studied for application in mobile robotics and gait analysis. Research on its kinematics involves the circle intersection method in analyzing foot trajectories and variations in steps, while dynamic modeling through the bond graph approach is related to the optimization of motor torque, joint stresses, and systems design [4]. After some limitations were found in the Klann mechanism, the Theo Jansen mechanism-Strandbeest-was chosen for its smooth motion. The research will involve

compressive load analysis compared with its load-carrying capacity to the standard wheel-based vehicle and control methods for such systems [6].

A detailed analysis of the linkages and the resulting motion is required to understand the kinematic behavior of these multi-legged walkers. Key parameters such as stride length, leg lift height, step synchronization, and energy efficiency must be considered to optimize performance. Achieving smooth and natural walking motion while minimizing mechanical complexity poses a challenge. Studies of four-, six-, and eight-legged walkers provide insights into the tradeoffs in the design of such robots. While an eight-legged offers greater stability, more complex synchronization of the legs is required, whereas a simpler design is achieved with a four-legged walker at the cost of some stability and energy efficiency. Six-legged walkers often strike a balance between stability and mechanical complexity, providing an efficient and stable gait.

After multiple studies were reviewed, it was found that a little simultaneous comparison of the four-, six-, and eightlegged mechanisms had been previously conducted. In existing research, we have found a gap in how leg variation in Jansen's walkers will affects the smoothness of walking. Most of the current research related to Theo Jansen robots is focused on specific designs; comparative work among four-, six-, and eight-legged models has not been fully presented. This paper discusses the comparison of the walking performance of the mentioned models, focusing on smoothness and efficiency. [5] [7] [8] [9]. In this paper, we have focused on how leg variation will affect smoothness by making comparisons on 8, 6 and 4-legged models. However, this paper has several limitations. Experimental comparisons between different legged designs (e.g., four-legged, sixlegged, and eight-legged) under various conditions were not

Published By: SciEn Publishing Group

provided, which would have strengthened the analysis. Although the importance of dynamic force analysis for improving energy efficiency is emphasized, concrete data or discussions on dynamic forces and their effects on performance are absent. The focus on theoretical design and optimization, with limited real-world testing or validation in challenging environments, reduces the practical relevance of the findings. Additionally, foot-ground interactions, critical for improving walking efficiency and stability, were not examined in detail. The simplified kinematic models may not fully capture the complexity of multi-degree-of-freedom systems in advanced robotics, limiting the generalizability of the results.

Furthermore, no discussion on material selection was included despite its importance for ensuring durability and performance in different environments. A thorough exploration of potential modern applications in robotics, along with a comparison to cutting-edge legged robots, would have highlighted the strengths and weaknesses of the mechanisms. Lastly, the discussion on optimization techniques was insufficient, as advanced methods that could further enhance the performance of the legged mechanisms were not explored. Addressing these limitations would make the research more comprehensive and applicable to real-world robotic systems. Kinematics analysis, CAD modeling and comparison of four-legged, six-legged, and eight-legged Theo Jansen mechanisms are presented in this paper.

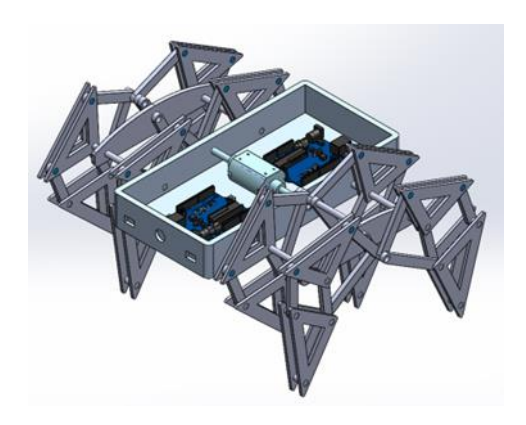


Fig. 1 Eight-legged CAD model in SolidWorks

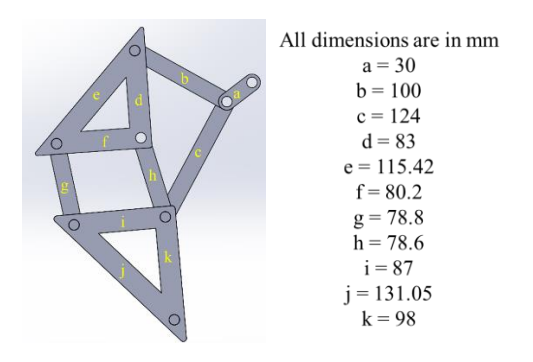


Fig. 1.1 Dimensions of the linkages for the CAD model

2. Methodology

This work has developed walkers based on the mechanism of Theo Jansen for an eight-, six-, and four-legged walking CAD model. In essence, our methodology has a number of key

stages, from initial analyses to final construction and validation of the CAD model (Fig. 1).

1. Model Design:

Following the mechanism developed by Theo Jansen, four-, six-, and eight-legged walking models were designed using SolidWorks software. Thereafter, each model is fabricated using identical links' dimensions for comparison consistency. The dimensions of the linkages are shown in Fig. 1.1, which are the same for all three models.

2. Kinematic Analysis:

The kinematic analysis of each model in movement is done on SolidWorks. Computation of joint angles links velocity and accelerations with angular directions for every instant of time during a walking cycle is done.

3. Motion Analysis:

A motor actuated the mechanism for each model in SolidWorks and then put through a motion analysis. The motor torque, angular velocity, and acceleration were considered in each of these models to understand the dynamic response.

4. Simulation:

Each of them was passed, in turn, through a simulation to determine how the respective walking would actually take place. For their part, the simulations quantified smoothness of continuous walking by using ground reaction forces, joint movements, and stride trajectory.

5. Comparative Study:

Some of the parameters considered in this regard included the velocity, variation in acceleration, and uniformity of stride-all, which helped in comparative studies based on walking smoothness, stability, motor torque, and efficiency.

6. Result Interpretation:

Kinematic and motion analysis data were therefore used to determine which model, in reality, had the smoothest walk under theoretical conditions.

3. Kinematics Analysis

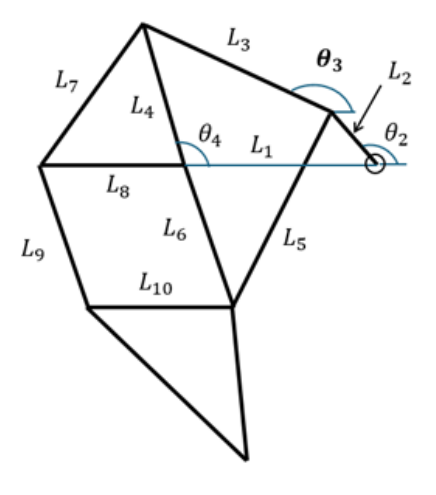


Fig. 2 All the linkages of one leg with length and angle of the model [1][10]

3.1 Kinematics (Loop $1 - L_1L_2L_3L_4$)

In solving kinematics with Fig. 2, information regarding the kinematics of the crank is considered and the kinematics is solved using the following equations which have been separated into three sub-analyses i.e. angular direction, angular velocity and angular acceleration.

3.1.1 Angular Direction Analysis:

Using the equation describing the position of the upper fourbar $L_1L_2L_3L_4$ (Fig. 3):

$$L_1 e^{i\theta_1} + L_4 e^{i\theta_4} = L_2 e^{i\theta_2} + L_3 e^{i\theta_3}$$
 (1.1)

where θ_I is the direction angle of link L₁. We can compute the unknown angles of θ_3 and θ_4 . [1]

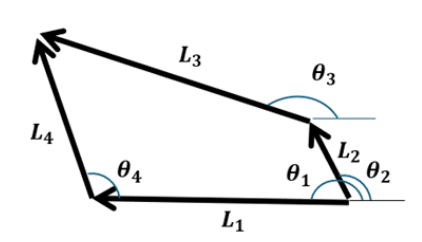


Fig. 3 Loop Closure Diagram, Loop 1 (L₁L₂L₃L₄) [1]

$$\theta_3 = \sin^{-1} \left[\frac{-b \pm \sqrt{b^2 - 4ac}}{2a} \right] \tag{1.2}$$

$$\theta_{3} = \sin^{-1} \left[\frac{-b \pm \sqrt{b^{2} - 4ac}}{2a} \right]$$

$$\theta_{4} = \cos^{-1} \left[\frac{L_{2} \cos \theta_{2} - L_{1} \cos \theta_{1} + L_{3} \cos \theta_{3}}{L_{4}} \right]$$
(1.2)

$$a = 4L_3^2(L_2^2 - 2L_1L_2\cos(\theta_1 - \theta_2) + L_1^2)$$

$$b = 4L_3(L_2\sin\theta_2 - L_1\sin\theta_1)(L_2^2 - 2L_1L_2\cos(\theta_1 - \theta_2) \\ + L_1^2 + L_3^2 - L_4^2)$$

$$\begin{split} c &= (L_2^2 - 2L_1L_2\cos(\theta_1 - \theta_2) + L_1^2 + L_3^2 - L_4^2)^2 \\ &- 4L_3^2(L_2^2\cos^2\theta_2 - 2L_1L_2\cos\theta_1\cos\theta_2 \\ &+ L_1^2\cos^2\theta_1) \end{split}$$

3.1.2 Angular Velocity Analysis:

Taking the time derivative of eq. (1.1) gives the equation describing the velocity of Loop 1: [1]

$$\dot{\theta}_4 i L_4 e^{i\theta_4} = \dot{\theta}_2 i L_2 e^{i\theta_2} + \dot{\theta}_3 i L_3 e^{i\theta_3} \tag{1.4}$$

$$\dot{\theta}_4 = \frac{\theta_2 L_2 \sin \theta_2 + \theta_3 L_3 \sin \theta_3}{L_4 \sin \theta_4} \tag{1.5}$$

$$\dot{\theta}_{4} = \frac{\dot{\theta}_{2}L_{2}\sin\theta_{2} + \dot{\theta}_{3}L_{3}\sin\theta_{3}}{L_{4}\sin\theta_{4}}$$

$$\dot{\theta}_{3} = \frac{\dot{\theta}_{2}L_{2}(\sin\theta_{2} - \tan\theta_{4}\cos\theta_{2})}{L_{3}(\cos\theta_{3}\tan\theta_{4} - \sin\theta_{3})}$$
(1.5)

3.1.3 Angular Acceleration Analysis:

Taking the time derivative of eq. (1.4) gives the equation describing the acceleration of loop 1: [1]

$$L_{4}(-\dot{\theta_{4}^{2}} + \ddot{\theta}_{4}i)e^{i\theta_{4}}$$

$$= L_{2}(-\dot{\theta_{2}^{2}} + \ddot{\theta}_{2}i)e^{i\theta_{2}}$$

$$+ L_{3}(-\dot{\theta_{3}^{2}} + \ddot{\theta}_{3}i)e^{i\theta_{3}}$$
(1.7)

$$\ddot{\theta}_{4} = \frac{B + L_{3}\ddot{\theta}_{3}\cos\theta_{3}}{L_{4}\cos\theta_{4}}$$

$$\ddot{\theta}_{3} = \frac{B\tan\theta_{4} - A}{L_{3}(\sin\theta_{3} - \cos\theta_{3}\tan\theta_{4})}$$
(1.8)

$$\ddot{\theta}_3 = \frac{B\tan\theta_4 - A}{L_3(\sin\theta_3 - \cos\theta_3 \tan\theta_4)} \tag{1.9}$$

Where.

$$A = L_2 (\dot{\theta}_2^2 \cos \theta_2 + \ddot{\theta}_2 \sin \theta_2) + L_3 \dot{\theta}_3^2 \cos \theta_3$$
$$- L_4 \dot{\theta}_4^2 \cos \theta_4$$
$$B = L_2 (-\dot{\theta}_2^2 \sin \theta_2 + \ddot{\theta}_2 \cos \theta_2) - L_3 \dot{\theta}_3^2 \sin \theta_3$$
$$+ L_4 \dot{\theta}_4^2 \sin \theta_4$$

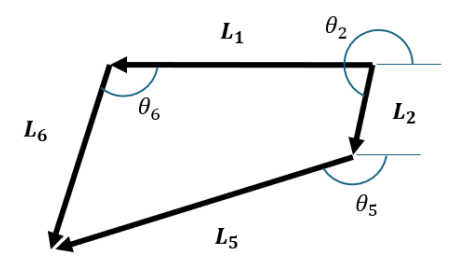


Fig. 4 Loop Closure Diagram, Loop 2 (L₁L₂L₅L₆) [1]

3.2 Kinematics Loop $2 - L_1L_2L_5L_6$

The derivations for kinematics are carried out in the same way as loop 1, but instead of taking links L₄ and L₃, links L₆ and L₅ are taken (Refer Fig. 4). The fundamental loop closure equation which defines loop 2 is given as follows:

$$L_1 e^{i\theta_1} + L_6 e^{i\theta_6} = L_2 e^{i\theta_2} + L_5 e^{i\theta_5}$$
 (2.1)

Using the methods discussed in Section 3.1 and equation (2.1) as a basis, the following equations which characterize the motion are obtained: [1]

3.2.1 Angular Direction Analysis:

$$a = 4L_5^2(L_2^2 - 2L_1L_2\cos(\theta_1 - \theta_2) + L_1^2)$$

$$b = 4L_5(L_2\sin\theta_2 - L_1\sin\theta_1)(L_2^2 - 2L_1L_2\cos(\theta_1 - \theta_2) + L_1^2 + L_5^2 - L_6^2)$$

$$\begin{split} c &= (L_2^2 - 2L_1L_2\cos(\theta_1 - \theta_2) + L_1^2 + L_5^2 - L_6^2)^2 \\ &\quad - 4L_5^2(L_2^2\cos^2\theta_2 - 2L_1L_2\cos\theta_1\cos\theta_2 \\ &\quad + L_1^2\cos^2\theta_1) \end{split}$$

$$\theta_5 = \sin^{-1} \left[\frac{-b \pm \sqrt{b^2 - 4ac}}{2a} \right] \tag{2.2}$$

$$\theta_6 = \cos^{-1} \left[\frac{L_2 \cos \theta_2 - L_1 \cos \theta_1 + L_5 \cos \theta_5}{L_6} \right]$$
 (2.3)

3.2.2 Angular Velocity Analy

$$\dot{\theta}_6 = \frac{\dot{\theta}_2 L_2 \sin \theta_2 + \dot{\theta}_5 L_5 \sin \theta_5}{L_6 \sin \theta_6} \tag{2.4}$$

$$L_6 \sin \theta_6 \tag{2.5}$$

K. S. M. J. Fahim et al. /SCSE Vol. 3, 2025, pp 713-718
$$\dot{\theta}_{5} = \frac{\dot{\theta}_{2}L_{2} \left(\sin\theta_{2} - \tan\theta_{6}\cos\theta_{2}\right)}{L_{5} \left(\cos\theta_{5} \tan\theta_{6} - \sin\theta_{5}\right)} \qquad \qquad \theta_{9} = cos^{-1} \left[\frac{L_{6}\cos\theta_{6} - L_{8}\cos\theta_{8} + L_{10}\cos\theta_{10}}{L_{9}}\right]$$

(3.3)

3.2.3 Angular Acceleration A

$$A = L_2 \left(\dot{\theta}_2^2 \cos \theta_2 + \ddot{\theta}_2 \sin \theta_2 \right) + L_5 \dot{\theta}_5^2 \cos \theta_5$$
$$- L_6 \dot{\theta}_6^2 \cos \theta_6$$

$$-L_6\theta_6^2\cos\theta_6$$

$$B = L_2(-\dot{\theta}_2^2\sin\theta_2 + \ddot{\theta}_2\cos\theta_2) - L_5\dot{\theta}_5^2\sin\theta_5 + L_6\dot{\theta}_6^2\sin\theta_6$$

$$\ddot{\theta}_5 = \frac{B\tan\theta_6 - A}{L_5(\sin\theta_5 - \cos\theta_5\tan\theta_6)}$$
(2.6)
The derivation for the velocity an

$$\ddot{\theta}_{6} = \frac{B + L_{5}\ddot{\theta}_{5}\cos\theta_{5}}{L_{6}\cos\theta_{6}}$$
 (2.7)

where A and B represents the known variables in the equation. [1]

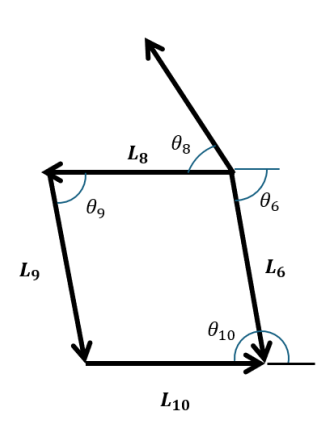


Fig. 5 Loop Closure Diagram, Loop 1 (L₁L₂L₃L₄) [1]

3.3 Kinematics Loop $3 - L_6L_8L_9L_{10}$

The equations of motion are obtained in a similar way as loop 1, except now the link terms L₁, L₂, L₃ and L₄ are substituted by L₈, L₆, L₁₀ and L₉, respectively. The basic loop closure equation that describes loop 3 (See Fig. 5) is:

$$L_{10}e^{i\theta_{10}} + L_6e^{i\theta_6} = L_8e^{i\theta_B} + L_9e^{i\theta_9}$$
 (3.1)

Based on eq. (3.1) and the methods used in Section 3.1, the following equations describing the kinematics are derived: [1]

3.3.1 Angular Direction Analysis:

$$L_8 e^{i\theta_8} + L_9 e^{i\theta_9} = L_6 e^{i\theta_6} + L_{10} e^{i\theta_{10}}$$
 (3.2)

$$a = 4L_{10}^2(L_6^2 - 2L_8L_6\cos(\theta_8 - \theta_6) + L_8^2)$$

$$b = 4L_{10}(L_6 \sin \theta_6 - L_8 \sin \theta_8)(L_6^2 - 2L_8L_6 \cos(\theta_8 - \theta_6) + L_8^2 + L_{10}^2 - L_9^2)$$

$$c = (L_6^2 - 2L_8L_6\cos(\theta_8 - \theta_6) + L_8^2 + L_{10}^2 - L_9^2)^2 - 4L_{10}^2(L_6^2\cos^2\theta_6 - 2L_8L_6\cos\theta_8\cos\theta_6 + L_9^2\cos^2\theta_9)$$

$$\theta_{10} = \sin^{-1} \left[\frac{-b \pm \sqrt{b^2 - 4ac}}{2a} \right] \tag{3.4}$$

The derivation for the velocity and acceleration will differ from the rest since all four links are mobile. Taking the time derivative of eq. (3.2) gives the equation describing the velocity of Loop 3: [1]

$$\dot{\theta}_8 i L_8 e^{i\theta_8} + \dot{\theta}_9 i L_9 e^{i\theta_9} = \dot{\theta}_6 i L_6 e^{i\theta_6} + \dot{\theta}_{10} i L_{10} e^{i\theta_{10}}$$
 (3.5)

Separating eq. (1.40) into its imaginary and real components, the unknown velocities can be solved by the following: [1]

$$= \frac{\dot{\theta}_6 L_6 \sin \theta_6 + \tan \theta_{10} (\dot{\theta}_6 L_8 \cos \theta_8 - \dot{\theta}_6 L_6 \cos \theta_6) - \dot{\theta}_6 L_8 \sin \theta_8}{L_9 (\sin \theta_{10} - \cos \theta_9 \tan \theta_{10})}$$

With the solution to the velocity of link L_9 the velocity of link L_{10} can be solved:

$$\dot{\theta_{10}} = \frac{\dot{\theta_8} L_8 \cos \theta_8 - \dot{\theta_6} L_6 \cos \theta_6 + \dot{\theta_9} L_9 \cos \theta_9}{L_{10} \cos \theta_{10}}$$
(3.7)

[1]

3.3.3 Angular Acceleration Analysis:

Taking the time derivative of eq. (3.5) gives the equation describing the acceleration of loop 3:

$$L_{8}(-\dot{\theta_{8}^{2}} + \dot{\theta_{8}^{"}}i)e^{i\theta_{8}} + L_{9}(-\dot{\theta_{9}^{2}} + \ddot{\theta}_{9}i)e^{i\theta_{9}}$$

$$= L_{6}(-\dot{\theta_{6}^{2}} + \ddot{\theta}_{6}i)e^{i\theta_{6}}$$

$$+ L_{10}(-\dot{\theta_{10}^{2}} + \ddot{\theta}_{10}i)e^{i\theta_{10}}$$
(3.8)

Separating eq. (1.43) into imaginary and real components, the unknown accelerations can be solved by the following:

$$\ddot{\theta}_{10} = \frac{\operatorname{Btan} \theta_{9} - A}{L_{10} (\sin \theta_{10} - \cos \theta_{10} \tan \theta_{9})}$$
(3.9)
$$\ddot{\theta}_{9} = \frac{B + L_{10} \ddot{\theta}_{10} \cos \theta_{10}}{L_{9} \cos \theta_{9}}$$
(3.10)
$$A = L_{6} (\dot{\theta}_{6}^{2} \cos \theta_{6} + \ddot{\theta}_{6} \sin \theta_{6}) + L_{10} \dot{\theta}_{10}^{2} \cos \theta_{10} - L_{8} (\dot{\theta}_{8}^{2} \cos \theta_{8} + \ddot{\theta}_{8} \sin \theta_{8}) - L_{9} \dot{\theta}_{9}^{2} \cos \theta_{9}$$

$$B = L_{6} (-\dot{\theta}_{6}^{2} \sin \theta_{6} + \ddot{\theta}_{6} \cos \theta_{6}) - L_{10} \dot{\theta}_{10}^{2} \sin \theta_{10} - L_{8} (-\dot{\theta}_{8}^{2} \sin \theta_{8} + \ddot{\theta}_{8} \cos \theta_{8}) + L_{9} \dot{\theta}_{9}^{2} \sin \theta_{9}$$

(3.6)

4. Results and Discussion

Angular direction, angular velocity, angular acceleration, and motor torque of the four-, six-, and eight-legged models have presented important differences regarding the smoothness of walking and mechanical efficiency. The eight-legged configuration can realize a smoother walk cycle compared with the other models.

The equations of angular direction, velocity, and acceleration are essential in understanding and optimizing the motion of mechanical systems. Angular direction provides precision orientation control, which is critical to stability in robotics. Angular velocity shows the speed of rotation, which helps optimize performance and prevent wear, while angular acceleration underlines the dynamic changes, thus allowing for efficient management of forces and torques. These parameters are basic to kinematic analysis, torque calculation, and predictive maintenance for smooth, efficient, and reliable operation of such applications as Theo Jansen-based walking mechanisms.

In the angular velocity graph (Fig. 9) for the eight-legged model, the legs moved consistently and uniformly; thus, the transition would be smoother at each stride of every leg. In In models of four and six legs, the fluctuation in angular direction was higher (Fig.10 & Fig. 11), meaning the movement was less stable, and the force would not be even during a walk.

The magnitudes of angular velocity and acceleration for the eight-legged model were highly uniform, with few peaks and troughs (Fig. 9). This smoother movement is indicative of a decrease in jerky motions compared to other models: six and four-legged models had much larger deviations, especially on the six-legged setup. There are more fluctuations in motor torque vs time graph in the six-legged model (points x1 to x5), as shown in Fig. 7. The four-legged model has less fluctuation than that of the six-legged model as shown (points y1 and y2) in Fig. 8, was once again worse in comparison to the eight-legged model regarding stability and uniformity.

The motor torque analysis also showed that the eight-legged model requires less variation of torque in order for smooth walking to take place (Fig. 6). Added legs helped to distribute more evenly the load and stresses that any individual joint or link would have to bear, making this model more efficient in terms of movement dynamics.

However, though the eight-legged model has demonstrated the best smoothness of walking, its advantage has also brought up some disadvantages. Since this model has more legs, building it requires more material; hence, it is heavier and more complex compared to the other configurations. The higher mass of the eight-legged model would need a more powerful motor for motion, which may increase energy consumption and generally increase complexity in the design. The four- and six-legged models are less smooth, simpler, and lighter and thus would require less powerful motors, hence, they would be more efficient from the material-energy point of view.

While the eight-legged model was much better in terms of smooth walking, it has disadvantages due to greater material usage and higher complications in the mechanical part and motor power. The choice between models must balance between the smoothness of the motion and other practical considerations as far as building complications are concerned, as well as weight and energy efficiency.

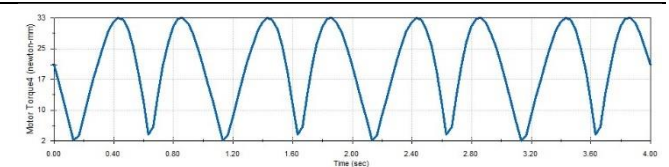


Fig. 6 Motor torque vs time graph of 8- legged model

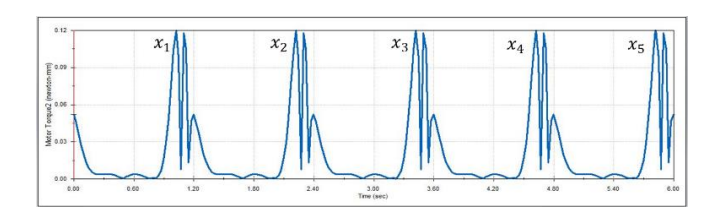


Fig. 7 Motor torque vs time graph of 6- legged model

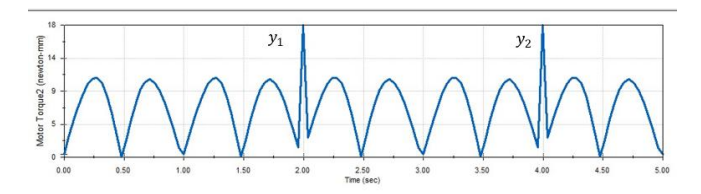


Fig. 8 Motor torque vs time graph of 4- legged model

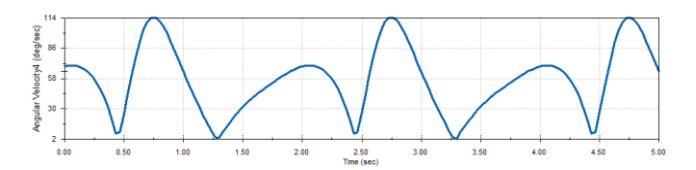


Fig. 9 Angular velocity vs time graph of 8- legged model

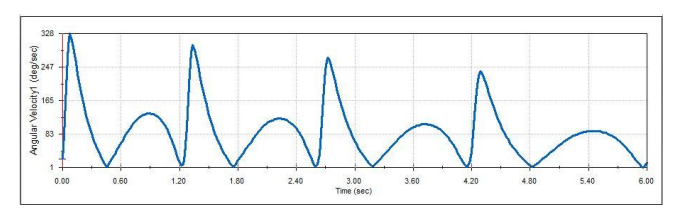


Fig. 10 Angular velocity vs time graph of 6- legged model

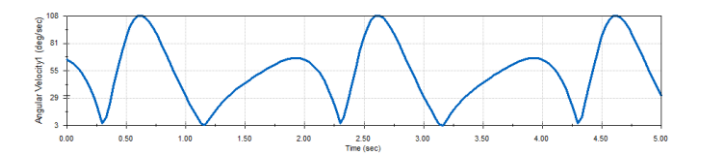


Fig. 11 Angular velocity vs time graph of 4- legged model

5. Conclusion

The authors of this paper compared the smoothness of the walks of the four-, six-, and eight-legged model mechanisms using kinematic and motion analysis with the mechanism created by Theo Jansen. It was revealed that the eight-legged model walked smoother due to a small angular deviation of direction, velocity, and acceleration, considering the reduction in the magnitude of variation of torque that results in more stable and fluent motion.

These advantages, however, have a few significant disadvantages in the eight-legged model. More legs require more material, which further leads to higher complexity and heavier mass that would require much more powerful motor action for its movement. In contrast, the four- and six-legged models are less smooth, simpler, and lighter, needing less powerful motors, hence more practical in applications.

Among them, the eight-legged model produced the best performance in the smoothness of the walk but, on the other hand, involves increased complexity with higher energetic demands and an increase of mass. Aluminum alloy, carbon fiber, glass fiber-reinforced plastic can be used for making prototypes to mitigate these drawbacks. In the light of such a proposal, the model selected could rest on these models for the proper application, keeping in view the smoothness, material constraints, and power of motors.

The present study analyzed the kinematics and torque-time behavior of the walking mechanisms; however, lifespan estimation, including fatigue and fracture analysis, was not considered because it requires detailed machine design, Finite Element Analysis, kinetics analysis and energy consumption that can be explored in future research. Effects of environmental factors can be further addressed in future research by machine learning and the creation of physical prototypes to experimentally analyze their effects, thus enhancing the robustness and practical applicability of the results.

References

- [1] Giesbrecht, D., Design and optimization of a one-degree-of freedom eight-bar leg mechanism for a walking machine., *Master thesis: University of Manitoba*, 2010 . https://mspace.lib.umanitoba.ca/items/42b246f4-4cad-4831-ad45-5c3d01ea7cb9
 (Date of access 10/04/2024)
- [2] K. Bhavsar, D. Gohel, P. Darji, J. Modi, and U. Parmar,

- 'Kinematic Analysis of Theo Jansen Mechanism-Based Eight-Leg Robot', in *Advances in Fluid Mechanics and Solid Mechanics*, 2020, pp. 75–82
- [3] M. Mohsenizadeh and J. Zhou, 'Kinematic Analysis and Simulation of Theo Jansen Mechanism', 11 2015. Conference: 2015 Early Career Technical Conference
- [4] L. Patnaik and L. Umanand, 'Kinematics and dynamics of Jansen leg mechanism: A bond graph approach', *Simulation Modelling Practice and Theory*, vol. 60, pp. 160–169, 2016.
- [5] S. Nansai, R. E. Mohan, N. Tan, N. Rojas, and M. Iwase, 'Dynamic Modeling and Nonlinear Position Control of a Quadruped Robot with Theo Jansen Linkage Mechanisms and a Single Actuator', *Journal of Robotics*, vol. 2015, pp. 1–15, 05 2015.
- [6] S. Patnaik, 'Analysis of Theo Jansen mechanism (Strandbeest) and its comparative advantages over wheel based mine escavation system', *IOSR J Eng*, vol. 5, no. 7, pp. 43–52, 2015.
- [7] J. S. Yucheng Liu Aaron Artigue and T. Chambers, 'Theo Jansen project in engineering design course and a design example', *European Journal of Engineering Education*, vol. 36, no. 2, pp. 187–198, 2011.
- [8] V. Dayanand, K. Attarde, and J. K. Sayyad, 'Development of Eight-legged Spider Robot Using Theo Jansen Mechanism', in 2024 6th International Conference on Energy, Power and Environment (ICEPE), 2024, pp. 1–6.
- [9] S. Nansai, N. Rojas, M. R. Elara, R. Sosa, and M. Iwase, 'On a Jansen leg with multiple gait patterns for reconfigurable walking platforms', *Advances in Mechanical Engineering*, vol. 7, no. 3, p. 1687814015573824, 2015.
- [10] K. Komoda and H. Wagatsuma, "A proposal of the extended mechanism for Theo Jansen linkage to modify the walking elliptic orbit and a study of cyclic base function," *Proceedings of the 7th Annual Dynamic Walking Conference (DWC'12)*, May 2012.